Eur Phys J C **40**, s02, 15–21 (2005)
Digital Object Identifier (DOI) 10.1140/epjcd/s2005-02-002-4

**EPJ C direct**
**electronic only**

*Scientific Note*

# Search with the CMS detector for Randall-Sundrum excitations of gravitons decaying into electron pairs

C. Collard[1], M.-C. Lemaire[2]

[1] LLR, Ecole Polytechnique, Palaiseau, France, e-mail: Caroline.Collard@poly.in2p3.fr
[2] SPP/DAPNIA, C.E. Saclay, France, e-mail: lemaire@hep.saclay.cea.fr

Received: 13 December 2004 / Revised: 16 February 2005 / Accepted: 18 February 2005
Published online: 25 April 2005 – 

**Abstract.** The sensitivity of the CMS experiment to the resonant production of massive Kaluza-Klein excitations of gravitons, expected in the framework of the Randall-Sundrum model, is studied. Full simulation and reconstruction are used to investigate this production followed by graviton decay to an $e^+e^-$ pair. For a Randall-Sundrum model with coupling parameter $c = 0.01$, the graviton excitations have weak couplings to Standard Model particles. For an integrated luminosity of 100 fb$^{-1}$, resonances can be discovered at the $5\sigma$ level for masses up to 1.8 TeV/$c^2$. Heavier resonances are accessible for larger values of the $c$ parameter, with a mass reach of 3.8 TeV/$c^2$ for $c = 0.1$.

## 1 Introduction

Theories with more than four space-time dimensions have been discussed in the context of unification of fundamental interactions [1]. In particular, string theories naturally incorporate quantum gravity with a spin-2 state identified with the graviton.These theories, however, generally imply unification of gauge and gravitational couplings close to the Planck scale, i.e. well beyond the reach of present and future colliders. The interest of extra spatial dimensions has been recently revived with models that lead to a gravity-related mass scale in the TeV range, relevant for particle physics at colliders [2,3].

The present study focusses on the Randall and Sundrum (RS) model [4] with only one extra dimension, with a compactification radius $r_c$. The gravity scale is given by

$$\Lambda_\pi = M_{\rm Pl}\, e^{-kr_c\pi}, \tag{1}$$

where $M_{\rm Pl}$ is the Planck mass and $k$ is the five-dimensional space-time curvature ($\sim M_{\rm Pl}$). The scale $\Lambda_\pi$ can be of the order 1 TeV/$c^2$ if $kr_c \simeq 11$ to 12 necessary to stabilize the scalar sector [5]. Therefore for $k \sim 10^{19}$ GeV, $r_c$ should be $\sim 10^{-32}$ m. The appearance of this four-dimensional gravity-related scale in turn eliminates the hierarchy problem.

Because of the small RS compactification radius, there are no deviations from Newton's law at experimentally accessible distances. On the other hand, massive Kaluza-Klein (KK) excitations of gravitons appear, with well separated masses given by

$$m_n = kx_n e^{-kr_c\pi}, \tag{2}$$

where $x_n$ is the $n^{\rm th}$ root of the Bessel function $J_1$.

In the RS model, these resonances are of the order of a TeV/$c^2$ and can be detected in collider experiments. Their couplings to Standard Model (SM) fermions and bosons are expected to be universal and the decay branching fractions depend essentially on the multiplicity of possible quantum states (spin, colour, flavour).

Two parameters control the properties of the RS model: the mass of the first KK graviton excitation $M_G = m_1$, and the coupling constant $c = k/M_{\rm Pl}$, which determines the graviton couplings and widths:

$$\Gamma_n = \rho m_n x_n^2 c^2, \tag{3}$$

where $\rho$ is a constant depending on the number of open decay channels.

Two theoretical constraints exist on these two parameters. The first one is given by the curvature bound $|R_5| = 20k^2 < M_5^2$ which yields $c < 0.1$ [4], where $R_5$ is the five-dimensional curvature scalar and $M_5 \sim M_{\rm Pl}$ is the fundamental five-dimensional Planck scale. The second constraint, $\Lambda_\pi < 10$ TeV, assures that no new hierarchy appears between $M_{\rm EW}$ and $\Lambda_\pi$. The best experimental constraints [6] on the Randall-Sundrum model come from Tevatron Run II data, which exclude $M_G$ up to 200 GeV/$c^2$ for $c = 0.01$ and 690 GeV/$c^2$ for $c = 0.1$.

The LHC will provide collisions with sufficiently high energy to open a new window in the $(M_G, c\,)$ parameter space. The main discovery channels come from the decay of the first KK excitation into electron or muon pairs. The

**Table 1.** The cross section times branching ratio $\sigma \times$ Br of the Drell-Yan $e^+e^-$ production predicted by the modified PYTHIA 6.215 and number of events generated in relevant mass intervals

| Process | Mass ($\mathrm{TeV}/c^2$) | $\sigma \times$ Br (fb) | Number of events |
|---|---|---|---|
| $pp \to \gamma, Z \to e^+e^-$ | 0.6-0.8 | 34.1 | 1000 |
| | 0.8–1. | 10.14 | 1000 |
| | 1.0–1.6 | 5.85 | 6000 |
| | 1.3–5.0 | 2.10 | 6000 |

present study deals with the $e^+e^-$ channel, which provides the best mass resolution at low coupling values where the width of the signal is dominated by the detector resolution. The signal is characterized by a clear resonance signature over a well-controlled Drell-Yan background, although the branching ratio for this channel is only 2 %.

The paper is organized as follows. In Sect. 2, signal and background generation is discussed as well as the special treatment of the internal Bremsstrahlung. In Sect. 3, the full simulation and reconstruction procedures are briefly described and the rôle of synchrotron radiation is investigated. The correction needed to deal with the electromagnetic calorimeter electronics saturation for very energetic electrons is also presented. The selection cuts are listed in Sect. 4. Finally, results are presented in Sect. 5.

## 2 Signal and background generation

At parton level, single gravitons can be produced at LHC via $q\bar{q} \to G$ or $gg \to G$. The cross sections for these processes are displayed in Fig. 1a. Each production mode gives a different angular distribution [7]. The expected signal is formed by an $e^+e^-$ pair, with both electrons balancing at very high $E_T$ and giving rise to a clear invariant mass peak (Fig. 1b). The SM background in this channel consists mostly of the Drell-Yan process: $q\bar{q} \to \gamma, Z \to e^+e^-$.

The generation of proton-proton collisions at 14 TeV centre of mass energy is done with PYTHIA 6.215 [8] modified to take into account the squared amplitude of the RS process as suggested by [9]. The CTEQ5L parton distribution function set [10] has been chosen. Internal Bremsstrahlung production was simulated with PHOTOS 2.03 [11]. The events were generated with the two electrons in the pseudorapidity region $|\eta| < 2.5$.

One thousand signal events were generated for each combination of mass and coupling shown in Fig. 1a. The numbers of generated events and the production cross sections of Drell-Yan $e^+e^-$ pairs in several relevant mass intervals, as predicted by PYTHIA, are listed in Table 1.

A K factor of 1.3 was used for the background, to take into account the higher order terms in the Drell-Yan cross section. This value comes from a CDF analysis [12] and is compatible with a K factor estimated in a fast simulation study [13]. No K factor was used for the signal.

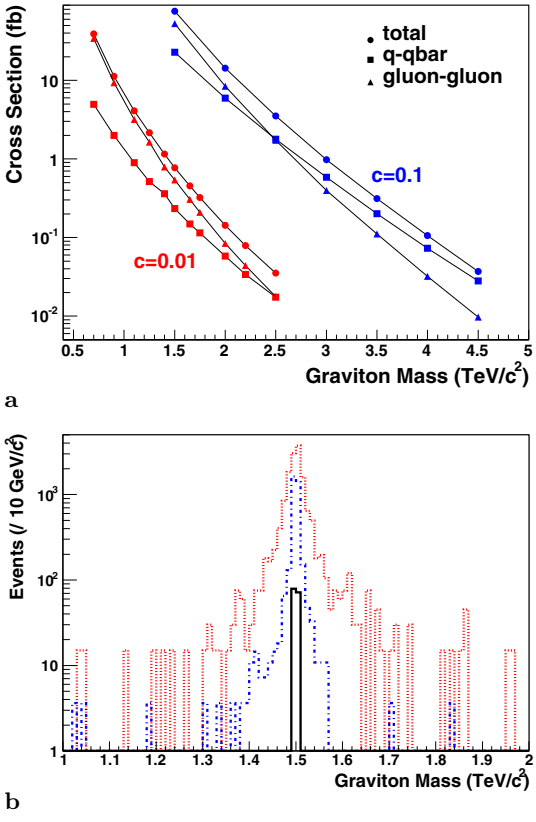


**Fig. 1. a** Cross section for the $pp \to G \to e^+e^-$ process (circles) for different values of $c$ ($c = 0.01$ and $c = 0.1$). The contributions of $q\bar{q}$ and gluon-fusion production mechanisms are displayed with squares and triangles respectively. **b** Invariant mass of the graviton at event generator level for a mass of 1.5 $\mathrm{TeV}/c^2$ and different couplings ($c = 0.01$, solid line; $c = 0.05$ dash-dotted line; $c = 0.1$, dotted line), corresponding to an integrated luminosity $\mathcal{L}$ of 100 $\mathrm{fb}^{-1}$

## 3 Event simulation and reconstruction

A detailed description of the CMS detector can be found elsewhere [14]. The simulation package CMSIM version 131 [15] based on GEANT3 was used to describe the detector geometry and materials. This package also handles the particle propagation and interactions with the detector. A careful treatment of the Bremsstrahlung in the tracker material and the synchrotron radiation in the 4T field of the CMS solenoidal magnet has been carried out. The synchrotron radiation was found to have a negligible effect on the electron energy compared to Bremsstrahlung. As an example, for 750 GeV electrons, the energy loss by synchrotron radiation is only about 10 GeV compared to 350 GeV loss from the charged particle from Bremsstrahlung in the tracker material.

The reconstruction was done with the CMS object-oriented reconstruction package ORCA version 7.2.2 [16]. This package handles all reconstruction tasks as well as the simulation of the detector response, the Level-1 trigger [17] and High Level Trigger [14]. Because their effect is

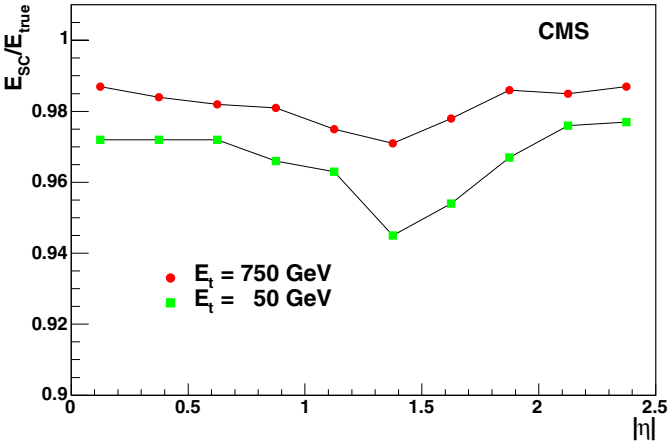


**Fig. 2.** Dependence on $|\eta|$ of the ratio $E_{\rm SC}/E_{\rm true}$

considered to be negligible for this analysis, pile-up events have not been included.

The Level-1 trigger has a 100 % efficiency for the channel under study. At Level 2.5 [14], the $e^{\pm}$ electromagnetic calorimeter (ECAL) clusters are required to match with hits in the pixel detector. This condition removes most of the photons from the electron candidate sample. The efficiency after the Level 2.5 selection is 99 %.

### 3.1 Electron Cluster reconstruction

The two electrons are reconstructed in the ECAL as 'Super-Clusters" using the "Island algorithm" [18] within the barrel and endcap fiducial regions ($|\eta| < 1.4442$ or $1.566 < |\eta| < 2.5$). The energy loss in the preshower is taken into account for endcap Super-Cluster reconstruction. A correction based on the fraction (H/E) of the Super-Cluster energy measured in the hadron calorimeter (HCAL) is applied to correct for the small energy loss from shower leakage beyond the ECAL. This correction improves the graviton mass resolution by about 8%.

A few per cent dependence on $\eta$ of the ratio of the measured Super-Cluster energy $E_{\rm SC}$ to the generated energy $E_{\rm true}$ is displayed in Fig. 2. This behaviour originates from the variation of tracker material thickness [18]. An additional smaller effect (0.6%) comes from the geometry of the calorimeter. In this analysis, a correction with 10 bins in $|\eta|$ is applied to bring the $E_{\rm SC}/E_{\rm true}$ ratios back to unity. This correction improves the resolution on the graviton reconstructed mass. These correction fa ctors were found to be independent of $E_{\rm T}$ between 250 to 1800 GeV, but they differ significantly from the values derived for $E_{\rm T} = 50$ GeV (Fig. 2).

### 3.2 The electronics saturation correction

For very energetic electrons, saturation occurs in the barrel ECAL electronics because of the limited dynamical range of the multi-gain-pre-amplifier [19]. A crystal light yield of 6 photo-electrons/MeV results in the most pessimistic limit for saturation, for energy deposits above 1.25 TeV. For the average value of the crystal light yield (4.5 photo-electrons/MeV), the saturation threshold is 1.7 TeV. This effect becomes visible for very large graviton masses. A simple correction of the energy $E_1$ measured in the most energetic crystal was applied based on the correlation (Fig. 3) between $E_1$ and the energy deposited in the least energetic corner of 5 crystals ($Red_5 = E_9 - E_4$, where $E_9$ and $E_4$ are the energies in the most energetic 3 $\times$ 3 and 2 $\times$ 2 crystal arrays).

A linear correlation is observed between $Red_5$ and $E_1$ over the full energy range. A fit restricted to low energy data (in absence of saturation) is performed. In the most pessimistic case of saturation (at 1.25 TeV), the fit performed on the range $Red_5 < 75$ GeV gives $E_1 = 11.98\ Red_5$. If the saturation occurs at higher values, for example at 1.7 TeV, a fit on the range $Red_5 < 115$ GeV gives $E_1 = 12.04\ Red_5$. The energy resolution after correction is 18 %, 12 % and 11 % for $E_1$, $E_{25}$ (the energy of the 5x5 crystal array) and $E_{\rm SC}$ respectively.

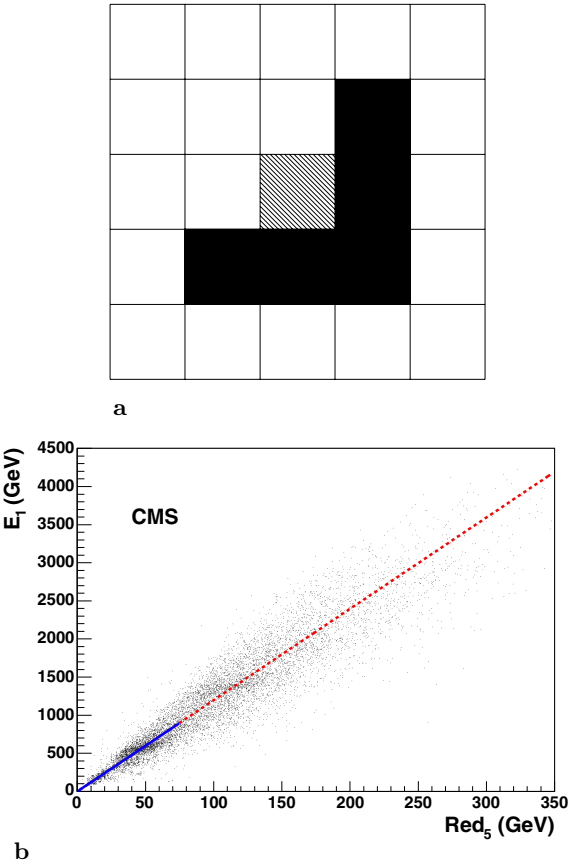


**Fig. 3. a** Definition in a 5 by 5 crystal tower of $E_1$ as the energy of the centre (hatched) crystal and of $Red_5 = E_9 - E_4$ as the energy of the 5 crystals in black. **b** Correlation between $E_1$ and $Red_5$, without simulation of saturation effects. The solid and dotted lines correspond respectively to the range used for the fit and its extrapolation

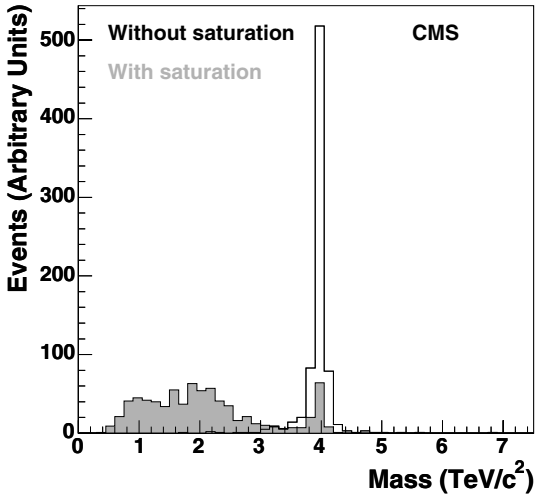


a

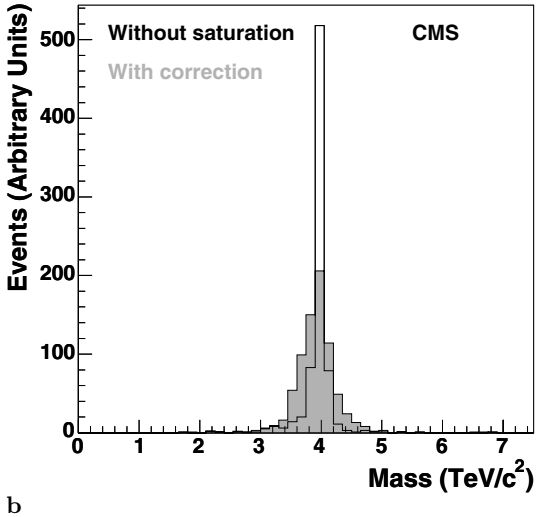


b

**Fig. 4.** The empty histograms represent the reconstructed graviton mass if no saturation occurs (signal of 4 TeV/$c^2$ with a coupling $c = 0.1$). The shaded histograms represent the reconstructed mass with the effect of the saturation at 1.25 TeV before **a** and after **b** the corrections

The effects of saturation and of the correction are shown for a graviton mass of 4 TeV/$c^2$ in Fig. 4. The $e^{\pm}$ pseudorapidity $\eta$ is not affected by the saturation of the crystal energy.

## 4 Event selection

The events must satisfy the trigger conditions (Sect. 3) up to the Level 2.5. Each Super-Cluster must have $E_T$ greater than 100 GeV and the two Super-Clusters with the highest $E_T$ are selected as electron candidates. The main backgrounds at this level are due to QCD jet-jet, $\gamma$-jet and e-jet events. The selection cuts, listed below, are based on the reconstruction of two very energetic and isolated electrons in the final state.

- In order to reduce the background coming from jets, the two Super-Clusters must be isolated in the electromagnetic calorimeter. The isolation criterion is based on the sum of the transverse energies deposited in clusters within a cone of opening radius $\Delta R = \sqrt{(\Delta\eta)^2 + (\Delta\phi)^2}$ centred around and excluding the electron candidate. The electron candidate is isolated if, in a cone of $\Delta R = 0.5$, the sum is below 2 % of the transverse energy of the Super-Cluster. This cut has an efficiency of 92.7 % for a 1.5 TeV/$c^2$ graviton mass.
- The background from isolated charged hadrons is eliminated with a cut on the hadronic energy fraction ($H/E$). The condition $H/E < 0.1$ keeps a signal efficiency of 99.2 % while a very small fraction ($< 0.4\%$) of the charged hadron pairs remains.
- The selection of electrons uses full track reconstruction, seeded by the pixel hits obtained at the matching step (Level-2.5 trigger). An efficiency of 98.2 % is achieved for the signal when at least two hits in the tracker are required for the reconstruction of the two charged particle tracks. This selection rejects most of the neutral particle final states. On a generated $\pi^0$ pair sample, 1.4 % of the events remain after the selection. Only 0.1 % of the $G \to \gamma\gamma$ events are kept.

The huge QCD backgrounds are efficiently rejected by these cuts. The only relevant background is formed by Drell-Yan $e^+e^-$ pairs.

## 5 Results

### 5.1 Significance

The graviton invariant mass is reconstructed from the two Super-Clusters. For each value of the generated graviton mass, the corresponding peak in the reconstructed mass spectrum is fitted with a Gaussian. A $\pm 3\sigma$ mass window is defined around the fitted peak to compute the numbers of signal and background events expected, $N_S$ and $N_B$. The numbers $N_S$ and $N_B$ are given for an integrated luminosity $\mathcal{L} = 100$ fb$^{-1}$ in Tables 2 and 3 for $c = 0.01$ and $c = 0.1$, respectively. Figure 5 shows the signal, for three mass hypotheses, 1.5, 1.75 and 2.0 TeV/$c^2$ for $c = 0.01$, and background for $\mathcal{L} = 100$ fb$^{-1}$. Figure 6 shows the signal and the background for two different cases: $M_G = 1.5$ TeV/$c^2$, $c = 0.01$ and $M_G = 3.5$ TeV/$c^2$, $c = 0.1$.

The significance is evaluated with the formula [20]:

$$S = 2(\sqrt{N_S + N_B} - \sqrt{N_B}). \quad (4)$$

With $\mathcal{L} = 100$ fb$^{-1}$, a $5\sigma$ discovery can be achieved up to 1.8 TeV/$c^2$ for $c = 0.01$ and to 3.8 TeV/$c^2$ for $c = 0.1$ (Fig. 7).

The discovery region in the plane of the coupling parameter $c$ and the graviton mass is given in Fig. 8. The present performance is very similar to what was found in the previous fast simulation of the CMS Collaboration [13] as well as in the results from the ATLAS Collaboration [7].

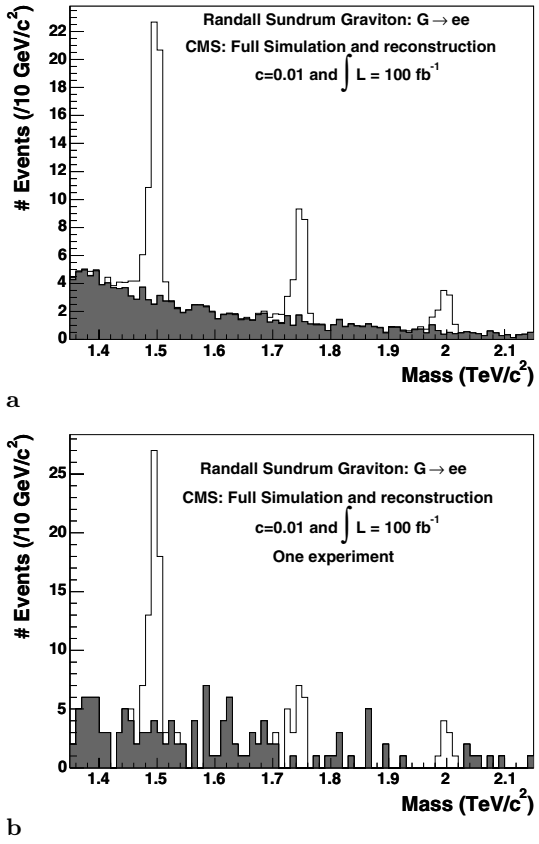


**Fig. 5.** Reconstructed invariant mass distribution for a Randall-Sundrum graviton decaying into an $e^+e^-$ pair. Three mass hypotheses 1.5, 1.7 and 2.0 TeV/$c^2$ are displayed over the background for $c = 0.01$ and $\mathcal{L} = 100$ fb$^{-1}$ : **a** large statistics, **b** single experiment

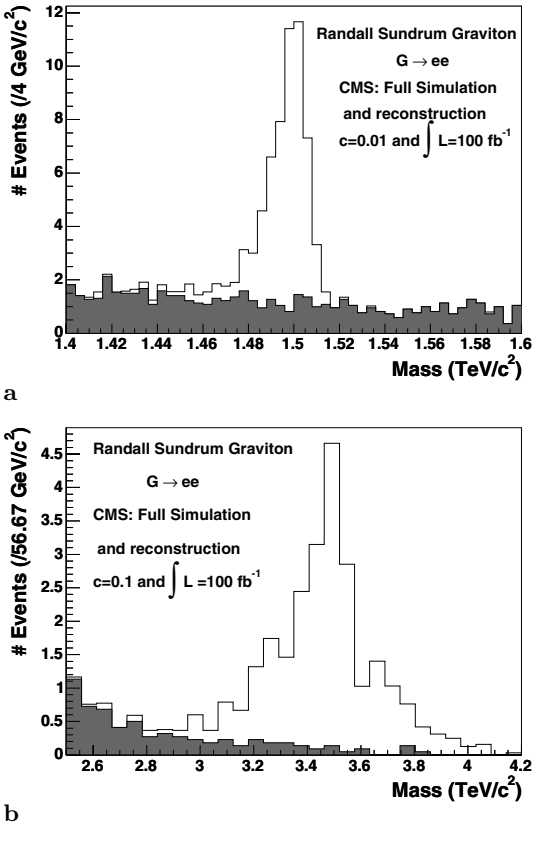


**Fig. 6.** Reconstructed invariant mass distribution for a Randall-Sundrum graviton decaying into an $e^+e^-$ pair. The signal is displayed over the background for $M_{\rm G} = 1.5$ TeV/$c^2$, $c = 0.01$ (a) and $M_{\rm G} = 3.5$ TeV/$c^2$, $c = 0.1$ (b) and $\mathcal{L} = 100$ fb$^{-1}$

**Table 2.** The numbers of signal and background events expected for $\mathcal{L} = 100$ fb$^{-1}$ and for $c = 0.01$

| M (GeV/$c^2$) | Mass window (TeV/$c^2$) | $N_S$ | $N_B$ | $S$ |
|---|---|---|---|---|
| 700 | 0.69–0.71 | 2518 | 284 | 72.2 |
| 900 | 0.89–0.91 | 800 | 100 | 40.0 |
| 1100 | 1.08–1.11 | 236 | 40 | 20.6 |
| 1250 | 1.23–1.27 | 133 | 28.2 | 14.8 |
| 1400 | 1.38–1.42 | 65.8 | 14.0 | 10.4 |
| 1500 | 1.48–1.52 | 46.7 | 9.85 | 8.8 |
| 1650 | 1.64–1.67 | 26.3 | 5.68 | 6.5 |
| 1750 | 1.73–1.77 | 18.6 | 4.63 | 5.3 |
| 2000 | 1.97–2.02 | 8.45 | 3.13 | 3.3 |
| 2200 | 2.17–2.23 | 4.47 | 1.41 | 2.5 |
| 2500 | 2.47–2.53 | 1.78 | 0.77 | 1.4 |

**Table 3.** The numbers of signal and background events expected for $\mathcal{L} = 100$ fb$^{-1}$ and for $c = 0.1$

| M (GeV/$c^2$) | Mass window (TeV/$c^2$) | $N_S$ | $N_B$ | $S$ |
|---|---|---|---|---|
| 2000 | 1.92–2.07 | 856 | 8.8 | 52.9 |
| 2500 | 2.39–2.59 | 204 | 3.45 | 25.1 |
| 3000 | 2.83–3.15 | 55.3 | 1.41 | 12.7 |
| 3500 | 2.89–4.02 | 23.4 | 2.32 | 7.1 |
| 4000 | 3.21–4.62 | 7.7 | 1.18 | 3.8 |

## 5.2 Systematic studies

A possible source of systematic uncertainty is the difference of normalization factors $E_{\rm SC}/E_{\rm true}$ as a function of $\eta$ between the high $E_{\rm T}$ and the 50 GeV $E_{\rm T}$ electron sample (Fig. 2). No significant change on the limit is observed here. If the low energy calibration is included, the fitted mass is shifted upward by 1–2%. Another systematic uncertainty may result from the choice of parton distribution functions. Changing from CTEQ5L to CTEQ6 [21] and MRS2001 [22] (from LHAPDF [23] library) leads to upward shifts of the limits by 105 and 112 GeV/$c^2$, respectively at low coupling $c = 0.01$, and 80 and 20 GeV/$c^2$ at high coupling $c = 0.1$. Varying the $Q^2$ scale in the structure functions from the default PYTHIA value $Q^2 = {M_{\rm G}}^2$ between 0.25 and 4 ${M_{\rm G}}^2$ yields limit variations of $\pm$ 20 GeV/$c^2$ for $c = 0.01$.

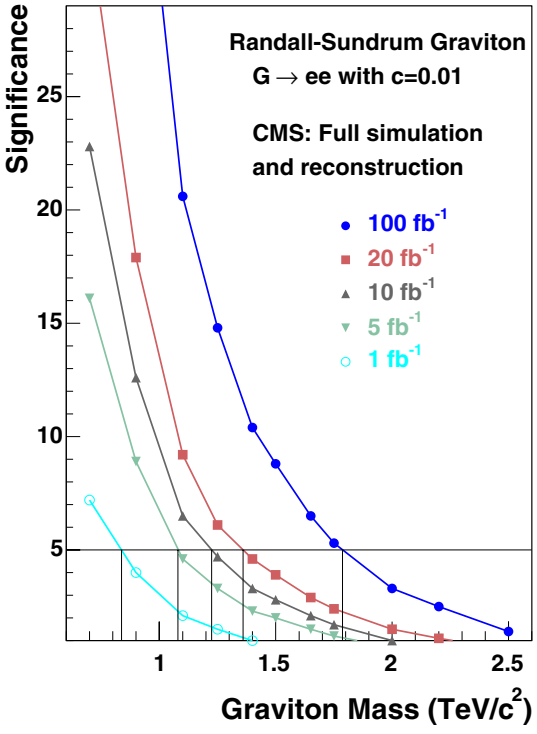


a

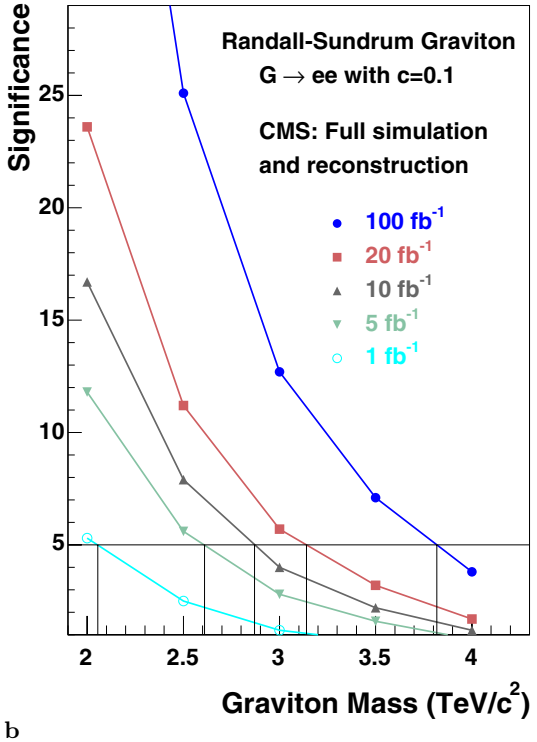


b

**Fig. 7.** Expected statistical significance for a Randall-Sundrum graviton decaying into an electron pair as a function of its mass. The results are displayed for two values of the coupling parameter $c = 0.01$ (a) and $c = 0.1$ (b). The various curves correspond to different integrated luminosities (from 1 to 100 $\text{fb}^{-1}$)

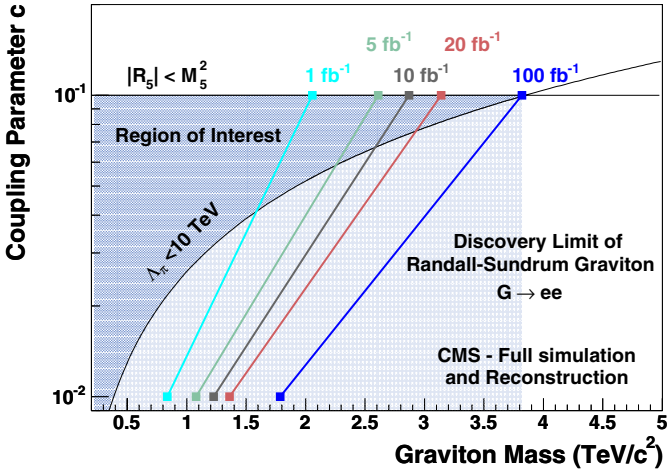


**Fig. 8.** Reach of the CMS experiment in the search for the Randall-Sundrum graviton decaying into an $e^+e^-$ pair as a function of the coupling parameter $c$ and the graviton mass. The various curves are labelled by the corresponding integrated luminosities. The left part of each curve is the region where the significance exceeds $5\sigma$. The shaded part corresponds to the theoretically preferred region (region of interest)

## 6 Conclusions

In this paper, results of a full simulation and reconstruction analysis on Randall-Sundrum graviton excitations are presented with the CMS detector. For a small value of the coupling $c = 0.01$, the $5\sigma$ discovery reach is 1.8 TeV/$c^2$ for $\mathcal{L} = 100$ $\text{fb}^{-1}$. Larger values of coupling ($c = 0.1$) give access to heavier gravitons. The electron saturation effect which occurs at these energies has been corrected for. The $5\sigma$ discovery reach is 3.8 TeV/$c^2$ for $c = 0.1$ and $\mathcal{L} = 100$ $\text{fb}^{-1}$. With this luminosity, the whole region of interest defined by the theoretical constraints is accessible with the CMS detector. Potential sources of systematic errors have been studied. The discovery reach is found to be stable to within about 100 GeV/$c^2$.

*Acknowledgements.* We would like to acknowledge E. Perez, N. Lahrichi, M. Besançon, T. Sjöstrand and M. Spira for fruitful discussions about the cross section behaviour and its implementation. We warmly thank the conveners of the PRS e/$\gamma$ and SUSY/BSM groups and the referees of this paper who provided useful comments and suggestions. We also acknowledge the LLR and Saclay groups for their support. Particular thanks are due to C. Charlot and Y. Sirois for their advice and stimulation throughout the present effort, J. Rander and the CMS editorial board for helpful comments on the present paper. Caroline Collard acknowledges the financial support provided through the European Community's Human Potential Programme under contract HPRN-CT-2002-00326, PRSATLHC.

## References


1. M. Besançon, C. R. Physique **4**, 319 (2003) and references therein
2. N. Arkani-Hamed, S. Dimopoulos, G. Dvali, Phys. Lett. B **429**, 263 (1998)
3. I. Antoniadis, K. Benakli, M. Quiros, Phys. Lett. B **331**, 313 (1994); I. Antoniadis, K. Benakli, M. Quiros, Phys. Lett. B **460**, 176 (1999); G. Azuelos, G. Posello, Kaluza-Klein Excitations of Gauge Bosons in the ATLAS Detector. Les Houches 2001, Physics at TeV colliders (2001) 121 and hep-ph/0204031
4. L. Randall, R.Sundrum, Phys. Rev. Lett. **83**, 3370 (1999); L. Randall, R. Sundrum, Phys. Rev. Lett. **83**, 4690 (1999)
5. W.D. Goldberger, M.B. Wise, Phys. Lett. B **475**, 275 (2000)
6. E. Kajfasz, Search for Extra-Dimensions at $p\bar{p}$ and ep Colliders. ICHEP 2004, Beijing
7. B.C. Allanach, K. Odagiri, M.J. Palmer, M.A. Parker, A. Sabetfakhri, B.R. Webber, Exploring Small Extradimensions at the Large Hadron Collider. hep-ph/0211205
8. T. Sjöstrand, Comput. Phys. Commun. **82**, 74 (1994); T. Sjöstrand et al., Comput. Phys. Commun. **135**, 238 (2001) LU TP 00-30, hep-ph/0010017
9. J. Bijnens et al., Phys. Lett. B **503**, 341 (2001)
10. CTEQ Collaboration, H.L. Lai et al., Eur. Phys. J. C **12**, 375 (2000)
11. E. Barberio, Z. Was, Comput. Phys. Commun. **79**, 291 (1994)
12. CDF Collaboration, Phys. Rev. Lett. **87**, 131802 (2001)
13. C. Collard, M.-C. Lemaire, P. Traczyk, W. Wrochna, Prospect for Study of Randall-Sundrum Gravitons in the CMS Experiment. CMS NOTE 2002-050
14. CMS Collaboration, CERN/LHCC 2002-026, CMS TDR 6.2, CMS The Tridas Project Technical Design Report, Volume 2: Data acquisition and High-Level Trigger
15. CMS Collaboration, CMS Simulation and ReconstructionPackage. http://cmsdoc.cern.ch/cmsim/cmsim.html
16. CMS Collaboration, CMS OO Reconstruction. http://cmsdoc.cern.ch/orca/
17. CMS Collaboration, CERN/LHCC 2000-038, CMS TDR 6.1, CMS The Tridas Project Design Report, Volume 1: The Trigger Systems
18. E. Meschi, T. Montero, C. Seez, P. Vikas, Electron Reconstruction in the CMS Electromagnetic Calorimeter. CMS NOTE 2001-034
19. M. Raymond, J. Crooks, M. French, G. Hall, The MGPA Electronic Calorimerer Readout Chip for CMS. Proceeding of the 2003 LECC Conference, CERN-2003-006
20. S.I. Bityukov, N.V. Krasnikov, Mod. Phys. Lett. A **13**, 3235 (1998); S.I. Bityukov, N.V. Krasnikov, Nucl. Instrum. and Methods A **452**, 518 (2000)
21. J. Pumplin et al., JHEP **0207**, 012 (2002) hep-ph/0201195
22. A.D. Martin, R.G. Roberts, W.J. Ryskin, W.J. Stirling, Eur. Phys. J. C **4**, 463 (1998)
23. D. Bourilkov, Study of Parton Density Function Uncerntainties with LHAPDF and PYTHIA at LHC. hep-ph/0305126